ARTICLE

OBC
www.rsc.org/obc

Locked TASC probes for homogeneous sensing of nucleic acids and imaging of fixed *E. coli* cells

Shinsuke Sando,* Atsushi Narita, Toshinori Sasaki and Yasuhiro Aoyama*
Department of Synthetic Chemistry and Biological Chemistry, Graduate School of Engineering, Kyoto University, Katsura, Nishikyo-ku, Kyoto, 615-8510, Japan.
E-mail: aoyamay@sbchem.kyoto-u.ac.jp; Fax: +81-75-383-2767; Tel: +81-75-383-2766

Received 1st December 2004, Accepted 7th February 2005
First published as an Advance Article on the web 22nd February 2005

We have designed a second-generation TASC (target-assisted self-cleavage) probe. It is based on the switching-on of incorporated *cis*-acting DNAzyme activity upon the target-induced conformational change of the otherwise inactive off-target probes locked in an intrastrand base-paired hairpin geometry. With *E. coli* 16S ribosomal RNA-relevant oligonucleotides as targets, the locked TASC probe exhibits an allosteric factor of $k_{on}/k_{off} = 65$ and the sequence selectivity is high, in terms of single nucleotide difference, when particular sequence and length of targets are chosen. Preliminary experiments with fixed *E. coli* cells show that the locked TASC probe with a FRET pair can be used to image fixed *E. coli* cells.

Introduction

As the increasing volumes of DNA sequence information continue to reveal important genetic markers, there are greater demands for rapid and accurate nucleic acid sensing, especially at single nucleotide resolution.[1] Although a number of nucleic acid sensing strategies have been reported during the last decade,[2] most of them are applicable only to PCR-isolated/purified specimens as targets. These isolation/purification processes normally require cell membrane destruction, resulting in loss of the individual information of various cells, allowing only a mean genetic information of cell assemblies to be determined. Differences in the genetic sequence, the amount of transcripts, and the timing of transcription among various cells are vital information for our understanding of cell-based events such as cell–cell communication.[3] The development of a method that can be used for *in situ* (especially in-cell) nucleic acid sensing without destruction of the cell membrane is highly desirable.

"Non-enzymatic and reagent-free nucleic acid detection" is a conceptually new method which has recently gained much attention for rapid, simple, and *in situ* (in-cell) sensing.[4–7] The FISH (**f**luorescence ***in situ*** **h**ybridization) approach[5] using fluorescence-labelled hybridization probes has been widely used on the single cell level. A problem with this is post-hybridization washing; off-target (unbound) fluorescent probes must be carefully and thoroughly removed,[8] thus preventing the method from being used for homogeneous *in situ* sensing. Recently, Kool and co-workers have developed a new DNA/RNA-sensing method, known as QUAL (**qu**enched **au**toligating) based on proximity-dependent chemical ligation, which proceeds only when two probes bind to the target DNA/RNA side-by-side, with concomitant "light up" upon nucleophilic displacement.[6a] They succeeded in detecting DNA on a solid surface[6a] and in discriminating ribosomal RNA (rRNA) sequences in fixed and non-fixed *Escherichia coli* (*E. coli*) cells with single nucleotide resolution, without post hybridization washing.[6b–c] Molecular beacons (MBs) are also successful examples of in-cell nucleic acid imaging.[7] MBs are hairpin-shaped oligonucleotide probes with an essential loop domain complementary to target DNA/RNA and a FRET pair at the 5′ and 3′ ends. Upon binding to the target, MBs undergo opening of the hairpin structure (and hence the FRET pair) to restore fluorescence. In a recent study, RNase-resistant MBs were used to visualize distribution and transport of *oskar* mRNA in living *Drosophia melanogaster* oocytes.[7b] Despite such work, these methods have been confronted with difficulties in terms of sensitivity, with a maximum of one signal from each target (at best) in a stoichiometric manner. The next challenge in this area is the amplification of sensing signals under physiological (isothermal) conditions.

Catalytic molecular beacons (catMBs)[9] and signal-amplifying ribozymes,[10] in which DNA/RNAzyme activity is initially suppressed by the MB sequence embedded in the same strand, are promising candidates for amplified sensing of nucleic acids.[11] Binding to the target results in opening of the MB structure, activating the *trans*-acting DNA/RNAzyme, triggering the catalytic cleavage of target FRET-probes,[12,13] and ultimately leading to amplification of unquenched fluorescence signals over a stoichiometric level in homogeneous solution.[9,10] However, such a *trans*-acting system, requiring synchronized association of the DNAzyme and FRET probe on the target DNA/RNA, would be less suitable for sensing in the crowded in-cell environment. We reported the TASC (target-assisted self-cleavage) approach as a new concept for catalytic mix-and-read sensing.[14] The *cis*-acting TASC probes incorporating a DNAzyme function are intended to undergo Mg^{2+}-assisted, on-target strand cleavage with concomitant dissociation of the probe fragments from the target, thus allowing multiple-turnover self-cleavage under conditions of [probe] > [target], where the essential role of target is that of an allosteric effector. Catalytic self-cleavage should result in amplified fluorescence emission under isothermal and enzyme/reagent-free conditions. In principle, this is indeed the case.[14] For in-cell use, there are a couple of concerns. First, non-sensing or off-target self-cleavage of the probe in excess should be highly suppressed. The first-generation TASC probe is not satisfactory in this respect; it is flexible and still possesses a substantial off-target activity. Second, on the other hand, the conformation and hence the activity of the off-target probe might be affected by intracellular components in an unpredictable way. We are concerned here about conformational fixation of the probe by itself.[9,10] The present work aims at shedding light on these two concerns. We report here that the second-generation TASC probe having a hairpin-locked geometry exhibits a better allosteric (target-on/off) performance and can be used for rRNA imaging in *E. coli*.

DOI: 10.1039/b418078j

Results and discussion

Design of locked TASC probes

Probes **1**–**5** used here (Fig. 1) are fluorescence-labelled at the 5′-end. TASC probe **1**, designed along the concept previously reported[14] with a basic design principle of Wang *et al.*,[13b–d] is composed of a self-cleaving sequence containing a DNAzyme domain (green) and a ribonucleotide rA as a specific cleavage site (purple) and a target-binding sequence (blue), split into two parts ($^{5'}$X and $^{3'}$Y) (10 + 10 = 20 nucleotides), complementary to the accessible 326–347 region of 16S rRNA[15] of the *E. coli* K12 strain MG1655 or the corresponding 22-mer oligodeoxyribonucleotide (ODN1) as a target in blue (Fig. 1a).[16] Self-cleaving reactions were conducted in a Tris–HCl buffer (50 mM, pH 7.2) containing Mg^{2+} (25 mM) with [probe] = 1 μM and [target] = 5 (5-fold molar excess) or 0 μM at 37 °C and the reaction kinetics were analyzed on PAGE. Incubation of TASC probe **1** with target 22-mer ODN1 afforded two fragmented ODNs (one was a fluorescent 14-mer and the other was a nonfluorescent 41-mer). The PAGE-monitored self-cleavage of this probe in the absence and presence of target ODN1 with Mg^{2+} followed the first-order kinetics with $k_{obs}^{-} = 1.8 \times 10^{-3}$ min^{-1} and $k_{obs}^{+} = 5.0 \times 10^{-3}$ min^{-1}, respectively (Table 1). This poor allosteric activation factor of $k_{obs}^{+}/k_{obs}^{-} \cong 2.8$ is not surprising in view of the flexible nature of the probe[16] and may be compared with the relatively large allosteric activation of the previously reported c-*fos* targeting TASC probe.[14] This conflict may be explained in terms of intramolecular or intrastrand folding of the off-target probes. Prediction of the secondary structure based on the RNAfold program shows that the present TASC probe **1** forms no well-definable secondary, *i.e.*, internal hybridized structure,[16] while the previous c-*fos* targeting probe forms a stable intrastrand hairpin-lock structure with a total of *ca.* 15 bp (bp = base pair). Thus, the low off-target activity of the previous probe is due to an unexpected folding. The intrastrand folding or base-pairing depends on the base sequence of variable parts of the probe, particularly the "stem" parts, which are constructed on an arbitrary basis[16] and the target-binding domain which is complementary to the particular target in concern. Removal of such an ambiguous and target-dependent nature of the off-target activity of the first-generation TASC probe is the aim of the design of the second-generation TASC probes for more general use.

We thus designed locked TASC probes **2** and **3** with a (10 + 10) or (8 + 8) target-binding sequence, respectively, wherein a $^{5'}$AAAAAG$^{3'}$ sequence (red) was added to the 5′-end. They are designed to form an internal hairpin-locked structure (Fig. 1b or **A** in Scheme 1) *via* intramolecular 6-bp hybridization with the $^{5'}$CTTTTT$^{3'}$ sequence, shown in red in Fig. 1a, to switch off the DNAzyme activity as in catMBs[9] and signal amplifying ribozymes,[10] keeping the DNAzyme domain[17] (green) and the rA cleavage site (purple) away from each other to prevent the probe from undergoing self-cleavage. In the presence of the target, they become unlocked upon 20-bp (**2**) or 16-bp (**3**) target-probe hybridization (step a) to switch on the activity by bringing the DNAzyme and the rA moieties in an enforced proximity (**B**) and hence promote cleavage (step c) *via* activation (**C**) with Mg^{2+} (step b). The fragmented products in **D** would either leave the target (step d) or be expelled therefrom by the full-length probe in excess (*vide infra*), regenerating free target or target-probe complex **B**, respectively, to drive a catalytic cycle when [probe] > [target] (Scheme 1).

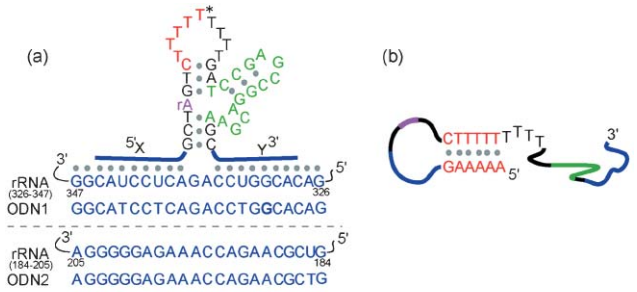

	5′X	Y3′	target rRNA site
TASC 1:	CCGTAGGAGT	GGACCGTGTC	326-347
locked TASC 2:	AAAAAGCCGTAGGAGT	GGACCGTGTC	326-347
locked TASC 3:	AAAAAGGTAGGAGT	GGACCGTG	328-345
TASC 4:	TCCCCCTCTT	GGACCGTGAC	184-205
locked TASC 5:	AAAAAGTCCCCCTCTT	GGACCGTGAC	184-205

Fig. 1 Sequences of TASC probes **1**–**5** and their targets. Illustration of (a) the target-probe complexation with gray dots representing base-pairing and (b) the internal hairpin-locked structure of locked probes **2**, **3** and **5** in the absence of target.

Table 1 Self-cleavage rate constants of 5′-fluorescein labelled TASC probes in the presence (k_{obs}^{+}) and absence (k_{obs}^{-}) of target together with derived allosteric factors (k_{obs}^{+}/k_{obs}^{-})[a]

Probe	Target	k_{obs}^{-}/min^{-1}[b]	k_{obs}^{+}/min^{-1}[b]	k_{obs}^{+}/k_{obs}^{-}
1	ODN1	1.8×10^{-3}	5.0×10^{-3}	2.8
2	ODN1	3.5×10^{-4}	4.3×10^{-3}	12.3
4	ODN2	1.2×10^{-3}	2.9×10^{-3}	2.4
5	ODN2	1.1×10^{-4}	7.1×10^{-3}	65

[a] [Probe] = 1 μM and [target] = 5 μM at 37 °C. [b] First-order rate constants were obtained as the slopes of ln P_f *vs* *t* plots where P_f is fraction of uncleaved probe and t = 0–120 min.

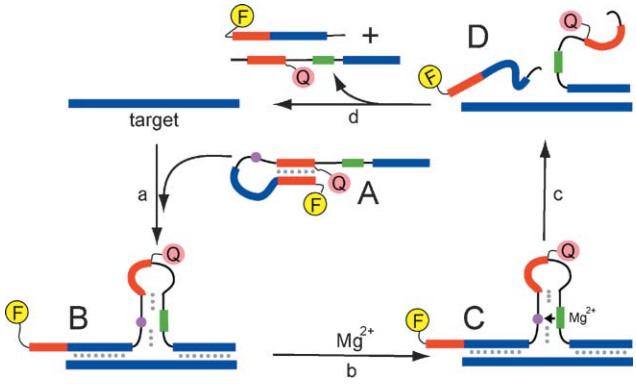

Scheme 1 Sensing scheme for locked TASC probe **2**, **3** and **5**, as specifically illustrated for FRET probe **3** having a FRET pair of fluorescein fluorophore (F) and dabsyl quencher (Q).

Melting behaviour of simplified model probes and their complexes

The validity of Scheme 1 was checked from the viewpoint of thermal stability in reference to the melting behaviours of model probes **a**–**d** in the presence and absence of target ODN **e** or **f** (Fig. 2a). The simplified model probes contain the essential partial structure of probe **2** with rA, if included, changed into non-cleavable deoxy-A (purple); such sequences as the DNAzyme domain are removed to avoid contribution of base-pairing arising therefrom. Target **e** is the same as ODN1, having a (10 + 10) probe-binding site. Target **f**, on the other hand, contains a shorter (8 + 8) binding site.

Melting curves were recorded by plotting the absorbance at 260 nm *vs* temperature for a probe or probe–target mixture in the same medium as for sensing experiments (*vide infra*), *i.e.*, in Tris–HCl (50 mM, pH 7.2) containing Mg^{2+} (25 mM). Probe **a** (2 μM strand concentration), having full lock domains (red), showed a melting curve (i) (Fig. 2c) with a midpoint of T_m = 45 °C for the hairpin-lock structure (**A** in Fig. 2b). This may also be taken as a measure of the thermal stability of such a structure (Fig. 1b and **A** in Scheme 1) of locked probes **2** and **3**. An equimolar (2 μM) mixture of probe **b**, having a full set

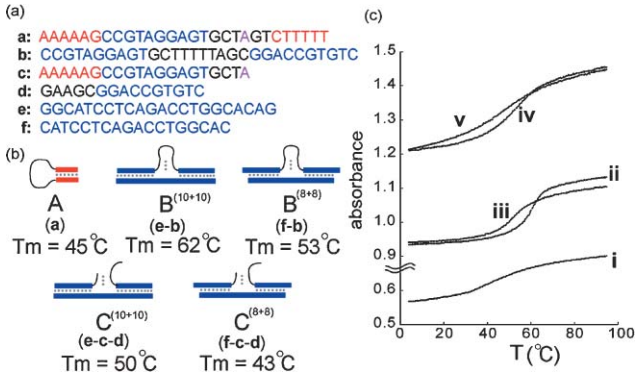

Fig. 2 Melting behaviour of simplified probe and target-probe systems; (a) sequences of simplified model probes **a**–**d** and targets **e** and **f**. The target binding domain, lock domain, and the A site (otherwise cleavable rA moiety in genuine TASC probes) are shown in blue, red, and purple, respectively; (b) schematic hybridization structures with melting temperatures of probe **a**, binary target–probe complexes **e–b** and **f–b**, and ternary complexes of target and probe fragments **e–c–d** and **f–c–d** in reference to the corresponding structures **A**, **B**, and **C** in Scheme 1; (c) melting curves for (i) probe **a**, (ii) an equimolar mixture of probe **b** and target **e** or (iii) **f**, and (iv) an equimolar ternary mixture of probes **c** and **d** and target **e** or (v) **f**. A pair of (10 + 10) and (8 + 8) curves [(ii) and (iii), and (iv) and (v)] are placed so as to have the same absorbance at low temperature to aid the comparison of melting temperatures.

of target-binding sequences (blue) and target **e** (10 + 10) or **f** (8 + 8), exhibited a melting curve (ii) or (iii) with $T_m = 62$ °C or 53 °C for the (10 + 10) or (8 + 8) target-probe complex $\mathbf{B}^{(10+10)}$ or $\mathbf{B}^{(8+8)}$ (Fig. 2b), respectively. These melting points must reflect the stabilities of the (10 + 10)- and (8 + 8)-binding **2**-ODN1 and **3**-ODN1 complexes (**B** in Scheme 1), respectively. Thus, from a thermal-stability consideration, probes **2** and **3** mostly exist in a 6-bp hairpin-locked structure with $T_m = 45$ °C (Fig. 1b and **A** in Scheme 1) at the experimental temperature (37 °C) but become unlocked upon hybridization with the target to give complex **B** (Scheme 1) with $T_m = 62$ or 53 °C.

The melting curve (iv) or (v) for an equimolar (2 μM) ternary mixture of probes **c** and **d**, respectively, having a fragmented target-binding sequence (blue) and target **e** or **f** is monophasic with a midpoint of $T_m = 50$ °C or 43 °C for the ternary complex $\mathbf{C}^{(10+10)}$ or $\mathbf{C}^{(8+8)}$ (Fig. 2c). This may also apply to the ternary complex formed upon on-target self-cleavage, referring to **D** in Scheme 1. While the observed melting temperatures are higher than the 37 °C at which sensing experiments were carried out, it is easily expected, judging from the less sharp melting behaviour, that partial melting or dissociation of the probe fragments (step d in Scheme 1) takes place at that temperature.

Self-cleavage reaction kinetics of locked TASC probes

The self-cleavage reactions of 5′-fluorescein labelled TASC probes were analyzed by fluorescence imaging of the 5′-fragment as the fluorescent cleavage product, as well as the uncleaved (unreacted) starting probe. The reactions follow the first-order kinetics and Mg^{2+} was essential. An example of the kinetic analysis is shown in Fig. 3 for probes **4** and **5** (*vide infra*). The first-order rate constants for locked probe **2** in the presence (5-fold molar excess) and absence of target ODN1 (Fig. 1) are summarized in Table 1. The off-rate (k_{obs}^-) is 5-times lower than that of the non-locked counterpart (probe **1**), while the on-rates are not surprisingly similar to each other; the allosteric activation factor (k_{obs}^+/k_{obs}^-) thus increases from 2.8 (probe **1**) to 12.3 (probe **2**). In order to shed light on the target-dependence, we prepared another set of probes, non-locked **4** and locked **5**, which target at an oligonucleotide (ODN2, Fig. 1) copying another (10 + 10) part (184–205 site) of the same 16S rRNA. Probes **5** and **2** (and **4** and **1** as well) differ only in the target-binding sequences. The kinetic data are shown in Fig. 3. The change in target from ODN1 to ODN2

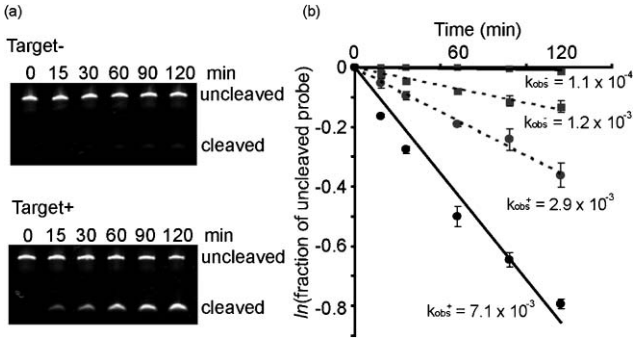

Fig. 3 (a) Self-cleavage reactions of locked TASC probe **5** (1 μM) as monitored by gel electrophoresis with fluorescence detection in the absence (Target-) and presence (5 μM) (Target+) of target ODN2; (b) first-order plots and derived rate constants for the self-cleavage reactions of probes **4** (dotted line) and **5** (solid line) (1 μM) in the presence (5 μM) (circle) and absence (square) of target ODN2. The error bar represents a standard deviation of data set obtained from at least three runs.

turns out to be slightly inhibitory on non-locked probes with respect to both k^+ and k^- ($k(\mathbf{4})^{ODN2+}/k(\mathbf{1})^{ODN1+} = 0.58$ and $k(\mathbf{4})^{ODN2-}/k(\mathbf{1})^{ODN1-} = 0.67$) without any big change in the allosteric factor $k(\mathbf{4})^{ODN2+}/k(\mathbf{4})^{ODN2-} = 2.4$ as compared with $k(\mathbf{1})^{ODN1+}/k(\mathbf{1})^{ODN1-} = 2.8$ (Table 1). For locked probes **2** and **5**, on the other hand, the effects are again slight but accelerating on k^+ and decelerating on k^- ($k(\mathbf{5})^{ODN2+}/k(\mathbf{2})^{ODN1+} = 1.7$ and $k(\mathbf{5})^{ODN2-}/k(\mathbf{2})^{ODN1-} = 0.31$); as a consequence, the allosteric factor is significantly enhanced to $k(\mathbf{5})^{ODN2+}/k(\mathbf{5})^{ODN2-} = 65$. Thus, on one hand, there is little doubt that the present lock strategy (Scheme 1) works in suppressing the off-target reactivity of the probe, while the net sensing accuracy in terms of k^+/k^- (≥ 10) is still delicately dependent on the target sequence. On the other hand, the origin of the non-negligible off-target reactivity of the probe in the neighbourhood of 10^{-4} min^{-1} should be further pursued in terms of lock-unlock equilibrium in reference to the melting temperature of $T_m = 45$ °C (Fig. 2) and intermolecular reactions.

Single nucleotide discrimination with locked TASC probe

Sequence selectivity of locked probe **2** in terms of single nucleotide discrimination was explored by using a one-base mismatched (T for G shown in bold in Fig. 1a) ODN1 as target. Locked TASC probe **2** having a (10 + 10) target-binding site with two intervening nucleotides turned out to be incapable of discrimination between fully matched (ODN1) and one-base mismatched targets ($k_{obs}^{(full)+} = 4.3 \times 10^{-3}$ min^{-1}, $k_{obs}^{(1-mis)+} = 3.4 \times 10^{-3}$ min^{-1}, and $k_{obs}^{(full)+}/k_{obs}^{(1-mis)+} \cong 1.3$) (Table 2). A one-base selectivity was achieved for target having a shorter (8 + 8) binding site copying the 328–345 site of 16S rRNA. In the presence of this full-match (8 + 8) target, probe **2** undergoes facilitated cleavage with $k_{obs}^{(full)+}$ in the expected 10^{-3} order (2.5×10^{-3} min^{-1}), while with the mismatch target with T for **G**, the cleavage rate constant ($k_{obs}^{(1-mis)+} = 2.9 \times$

Table 2 Self-cleavage rate constants of locked TASC probe **2** in the presence of fully matched ($k_{obs}^{(full)+}$) and one-base mismatched ($k_{obs}^{(1-mis)+}$) target oligonucleotides having either a (10 + 10) or (8 + 8) binding site[a]

Target ODN	$k_{obs}^{(full)+}/min^{-1}$ [b]	$k_{obs}^{(1-mis)+}/min^{-1}$ [b]	$k_{obs}^{(full)+}/k_{obs}^{(1-mis)+}$
(10 + 10)[c]	4.3×10^{-3}	3.4×10^{-3}	1.3
(8 + 8)[d]	2.5×10^{-3}	2.9×10^{-4}	8.6

[a] [Probe] = 1 μM and [target] = 5 μM at 37 °C. [b] First-order rate constants were obtained as the slopes of ln P_f *vs* *t* plots where P_f is fraction of uncleaved probe and t = 0–120 min. [c] Fully matched and one-base mismatched targets are 3′-GGCATCCTCAGACCTGGCACAG-5′ and 3′-GGCATCCTCAGACCTGTCACAG-5′, respectively. [d] Fully matched and one-base mismatched targets are 3′-CATCCTCAGACCTGGCAC-5′ and 3′-CATCCTCAGACCTGTCAC-5′, respectively.

10^{-4} min^{-1}) is essentially the same as the off-target rate constant ($k_{obs}^{-} = 3.5 \times 10^{-4}$ min^{-1}); the apparent one-base selectivity of $k_{obs}^{(full)+}/k_{obs}^{(1-mis)+} \cong 8.6$ may thus be taken as evidence for a high level of single nucleotide discrimination in the present system.

Fluorescence imaging of fixed *E. coli* cells

Fluorescence in-cell nucleic acid sensing requires automatic light-up upon target-probe hybridization. We devised a (8 + 8) FRET probe **3**^{FRET} having a dabsyl quencher (Q) at the asterisked T moiety (Fig. 1a) in the loop domain of probe **3**; Q would form a FRET pair with the fluorescein fluorophore (F) attached to the base-pairing partner A at the 5′-end in the hairpin-locked off-target ground state (**A** in Scheme 1). When the probe is bound to the target (328–345 site of rRNA, Fig. 1) with an expected conformational change (**B** in Scheme 1), FRET pair should be unlocked with concomitant emission of fluorescence due to opening of the hairpin-lock domain. For accuracy, the locked TASC probe should keep the off-target locked hairpin conformation in the cells (step a in Fig. 4) and should change into an active form only when binding to target RNA (step c). This is not *a priori* guaranteed, however, in the crowded[18] multi-component in-cell environment, where the structures of the probe and target may be affected by coexisting DNAs, RNAs and other macromolecules, or intramolecularly folded more closely.[19] The present target can be taken as an illustration. The target nucleotide sequence 328–345 of *E. coli* 16S rRNA (shown in blue in Fig. 4) is expected to be poorly accessible due to competing self-hybridization, wherein at least 9 (out of 18) nucleotides could form stable base pairs with nearby nucleotides to mask the target site, referring to the "non-accessible" form in Fig. 4. In these circumstances, "helper" ODNs can be used; the 3′-helper (3′-CCCTCCGTCGTCACCCCTTA-5′) and the 5′-helper (3′-GTCGGTGTGACCTTGACTCT-5′) are expected to bind to the flanking sites (308–327 and 346–365, respectively) adjacent to the target site (328–345) to open the latter, *i.e.*, to convert it from the non-accessible form to accessible (step b in Fig. 4).[20]

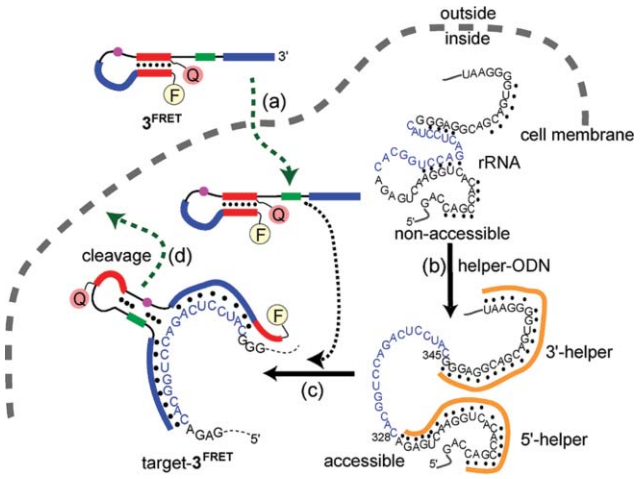

Fig. 4 Schematic illustration of the working mechanism of FRET TASC probe **3**^{FRET} in the *E. coli* cell. The locked probe enters the cell through permeabilized membrane (step a), where it hybridizes (step c) with 16S rRNA, assisted (step b) by helper ODNs in orange, with an open or accessible target site (nucleotides 328–345) in blue to give a cleavage-susceptible and FRET-free target-probe complex, followed by its catalytic cleavage (step d).

This is indeed the case. *E. coli* cells (K12 strain MG1655) were fixed with paraformaldehyde according to the literature protocols,[15a] washed once with PBS, and incubated with FRET locked TASC probe **3**^{FRET} (1 μM) at 37 °C in a Tris–HCl hybridization buffer (50 mM pH 7.2) containing Mg^{2+} (25 mM) and SDS (0.1%). The cell suspension was directly spotted on a glass slide without post-hybridization washing for fluorescence microscopic observation. In the absence of the helpers, the cells were nonfluorescent (Fig. 5a and Fig. 6a for confocal and wide-field microscopic images, respectively), showing that the probe still keeps a hairpin-locked, off-target conformation in the cells, as in solution.[21] In marked contrast, when the helper ODNs were present, the cells became fluorescent (Fig. 5b and Fig. 6b), indicating that sequence-selective hybridization of unlocked probe **3**^{FRET} and subsequent self-cleavage[22] took place exactly at the target site (step c in Fig. 4).[23]

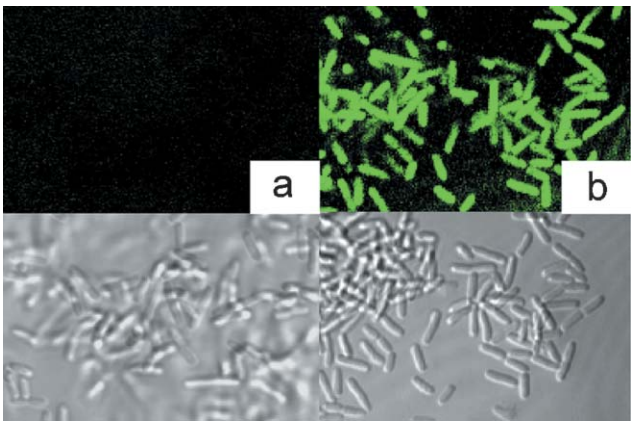

Fig. 5 Optical micrographs (bottom) and their confocal fluorescence images (top) of *E. coli* cells incubated for 6 h with FRET locked probe **3**^{FRET} in a Tris–HCl (50 mM, pH 7.2) buffer containing Mg^{2+} (25 mM) and 0.1% SDS (a) without or (b) with helper ODNs (10 μM each).

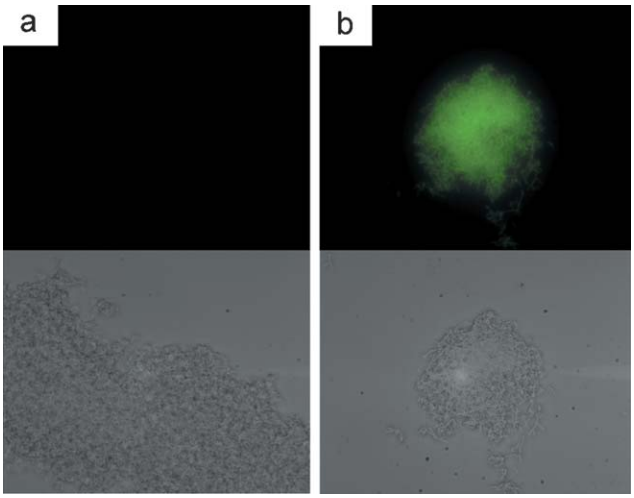

Fig. 6 Optical micrographs (bottom) and their wide-field fluorescence images (top) of *E. coli* cells incubated for 6 h with FRET locked probe **3**^{FRET} in a Tris–HCl (50 mM, pH 7.2) buffer containing Mg^{2+} (25 mM) and 0.1% SDS (a) without or (b) with helper ODNs (10 μM each).

Concluding remarks

In summary, the lock strategy gives rise to a sort of generality or versatility of the TASC (target-assisted self-cleavage) approach to the nucleic acid sensing. While it works relatively fine with $k_{on}/k_{off} = 65$ and a high level of single nucleotide discrimination for targets of particular sequence and length, the general efficiency in terms of allosteric factor of ≥10 still remains to be improved, particularly in view of catalytic or amplified sensing, by stabilizing the off-target lock structure (**A** in Scheme 1) as well as by geometrically manipulating the on-target DNAzyme action on the cleavage site (**B**). The rRNA imaging of *E. coli* cells may be taken as a sign of the potentiality of the dissociative TASC probes working in crowded intracellular environments.

At the same time, the fate of the sensing-responsible probe-fragment becomes a new concern. With these concerns taken in mind, we step toward further work for genetic sensing/imaging of the cells, which may have a variety of applications such as non-destructive detection of bacteria and viruses and *in vivo* selection of drugs.[24]

Experimental

Preparation of TASC probes

TASC probes with fluorescein labelling at the 5′-end were prepared on a DNA/RNA synthesizer (ABI 392, Perkin-Elmer) using phosphoramidites (Glen Research) of Bz-dA, ^{i}Bu-dG, dT, and Ac-dC, fluorescein, Ac-A-TOM as a source of rA, and, in case of FRET TASC probe **3**, dabsyl-dT as a FRET partner. The CPG solid support was incubated in 1.5 mL of a methylamine solution, prepared by mixing 1 volume of 40% aqueous methylamine (Fluka) and 1 volume of 33% ethanolic methylamine (Fluka), for 6 h at 35 °C to liberate the oligonucleotide with concomitant deprotection. The mixture was lyophilized to yield a yellow solid (orange solid in the case of FRET TASC probe), which was dissolved in 1 mL of 1 M tetrabutylammonium fluoride in THF (Sigma) and left at 50 °C for 10 min and at 35 °C for 6 h to be freed from the TOM protecting group. Addition of 1 mL of 1 M Tris buffer was followed by evaporation of most of THF and addition of another 1 mL of Tris buffer. The fully-deprotected TASC probes were purified on NAP-25 desalting column (Amersham), followed by electrophoresis on an 8% polyacrylamide denaturing gel containing 7 M urea. The TASC probes were extracted from the gel with 10 mL of H_2O overnight at 37 °C and then dialyzed using MWCO 1000 Float-A-Lyzer (Spectrum) in a large volume of H_2O. The solution was lyophilized to give TASC probes.

Analysis of self-cleavage reactions

Targets ODN1 and ODN2 were purchased from Qiagen. All of the reactions were carried out at [probe] = 1 μM in 100 μL of Tris–HCl buffer (50 mM, pH 7.2) containing $MgCl_2$ (25 mM) at 37 °C with [target] = 5 or 0 μM. The reaction was quenched at an appropriate time interval by mixing with 800 μL of cold ethanol. The mixture was stored at −80 °C for 30 min and then centrifuged at 9500 g for 30 min. The ethanol precipitates were dissolved in a 1 : 1 mixture of water (5 μL) and loading buffer (1 mM EDTA in formamide, 5 μL) and analyzed by electrophoresis (ATTO RAPIDAS AE-6200) on an 8% polyacrylamide denaturing gel containing 7 M urea. The reactions were monitored by fluorescence imaging. The yields of cleavage were assayed by referring to the relative fluorescence intensities of intact TASC probe and its fluorescent fragment after careful calibration with known concentrations of authentic specimen, using an ATTO densitograph AE-6920 equipped with a lane & spot analyzer, version 6. The first-order rate constants were obtained as slopes of *ln*(fraction of uncleaved probe) *vs* *t* plots in the conversion range indicated. Each data point was obtained as an average of at least three independent data sets and the goodness-of-fit of the line to the data points was evaluated by the correlation coefficient of $R > 0.97$ as the criterion for an acceptable fit.

Measurements of melting temperature

Oligonucleotides (2 μM each) were dissolved in a Tris–HCl buffer (50 mM, pH 7.2) containing $MgCl_2$ (25 mM). The mixture was heated for 5 min at 95 °C and cooled down slowly to 4 °C. The thermal denaturation profile was recorded on a UV-visible spectrophotometer UV-1650 PC (Shimazu) with a Peltier temperature controller. The absorbance of the sample was monitored at 260 nm from 4 °C to 90 °C with a heating rate of 1 °C min^{-1}. The T_m value was determined as the maximum in a plot of $\Delta A_{260}/\Delta T$ *vs* temperature.

Cell fixation

E. coli cells (K12 strain MG1655) were grown in 6 mL of LB broth at 37 °C until the optical density (OD_{600}) of the cell suspension became 0.5. Then, the suspension was quickly chilled on ice for 5 min and aliquots (1 mL) were taken into 1.5 mL eppen tubes. Cells were harvested by centrifugation at 9500 g for 5 min at 0 °C. After centrifugation, the supernatant was removed by pipetting and cells were washed once with 1 mL of PBS. For fixation, cells were resuspended in 1 mL of 4% paraformaldehyde (Aldrich) in PBS solution (filter sterilized, pH 8.0 adjusted by 1 N NaOH) and the suspension was stored for 1 h at room temperature. After fixation, the suspension was centrifuged at 9500 g for 5 min at 0 °C and the supernatant was removed by pipetting. Precipitated cells were washed once with 1 mL PBS. The fixed cells were resuspended in 1 mL of 50% ethanol and stored at −20 °C.

Fluorescence imaging of FRET TASC probe in fixed *E. coli* cells

A 167 μL portion of fixed cell suspension stocked in 50% ethanol, prepared according to the method described above, was taken into a 1.5 mL eppen tube and centrifuged at 9500 g for 5 min at 0 °C. The precipitated fixed cells were washed once with 100 μL PBS and resuspended in 100 μL of hybridization buffer of 50 mM Tris–HCl containing 25 mM $MgCl_2$ and 0.1% SDS with or without 3′/5′-helper oligonucleotide probes (10 μM each, final strand concentration). To the suspension was added FRET TASC probe **3** (1 μM, final strand concentration) and the mixture was incubated at 37 °C. A 3 μL portion of the mixture was taken after gentle centrifugation for optical and fluorescence micrography. Confocal and wide-field fluorescence images were obtained using Fluoview FV500 (Olympus) and IX70 fluorescence microscope (Olympus), respectively.

Acknowledgements

We thank Professor Y. Mori and Dr T. Yoshida of Kyoto University for fluorescence microscopy. This work was supported by Industrial Technology Research Grant Program from the New Energy and Industrial Technology Development Organization (NEDO) of Japan, and by Grant-in-Aid for Scientific Research on Priority Areas (C) "Genome Science" and also by Grant-in-Aids No. 16350087 and 16023230 from the Ministry of Education, Science, Sports and Culture, Japan.

References

1 (*a*) A. J. Schafer and J. R. Hawkins, *Nat. Biotechnol.*, 1998, **16**, 33; (*b*) R. M. Twyman, *Curr. Top. Med. Chem.*, 2004, **4**, 1423.
2 P. Y. Kwok and X. Chen, *Curr. Issues Mol. Biol.*, 2003, **5**, 43.
3 (*a*) I. Mihalcescu, W. Hsing and S. Leibier, *Nature*, 2004, **430**, 81; (*b*) C. H. Johnson, *Nature*, 2004, **430**, 23, and references therein.
4 For recent reports on PCR-free homogeneous nucleic acid sensing, see for example: (*a*) J. J. Storhoff, R. Elghanian, R. C. Mucic, C. A. Mirkin and R. L. Letsinger, *J. Am. Chem. Soc.*, 1998, **120**, 1959; (*b*) F. Patolsky, A. Lichtenstein and I. Willner, *J. Am. Chem. Soc.*, 2001, **123**, 5194; (*c*) Y. Xu, N. B. Karalkar and E. T. Kool, *Nat. Biotechnol.*, 2001, **19**, 148; (*d*) R. T. Ranasinghe, T. Brown and L. J. Browon, *Chem. Commun.*, 2001, 1480; (*e*) V. C. Rucker, S. Foister, C. Melander and P. B. Dervan, *J. Am. Chem. Soc.*, 2003, **125**, 1195; (*f*) A. Okamoto, K. Kanatani and I. Saito, *J. Am. Chem. Soc.*, 2004, **126**, 4820; (*g*) G. T. Hwang, Y. J. Seo, S. J. Kim and B. H. Kim, *Tetrahedron Lett.*, 2004, **45**, 3543; (*h*) J. Cai, X. Li, X. Yue and J. S. Taylor, *J. Am. Chem. Soc.*, 2004, **126**, 16324.
5 For recent reviews on the FISH technology, see: (*a*) A. Moter and U. B. Göbel, *J. Microbiol. Methods*, 2000, **41**, 85; (*b*) A. Lipski, U. Friedrich and K. Altendorf, *Appl. Microbiol. Biotechnol.*, 2001, **56**, 40; (*c*) J. M. Levsky and R. H. Singer, *J. Cell Sci.*, 2003, **116**, 2833.
6 (*a*) S. Sando and E. T. Kool, *J. Am. Chem. Soc.*, 2002, **124**, 2096; (*b*) S. Sando and E. T. Kool, *J. Am. Chem. Soc.*, 2002, **124**, 9686;

(*c*) S. Sando, H. Abe and E. T. Kool, *J. Am. Chem. Soc.*, 2004, **126**, 1081.
7 (*a*) S. Tyagi and F. R. Kramer, *Nat. Biotechnol.*, 1996, **14**, 303; (*b*) S. Tyagi, P. Bratu and F. R. Kramer, *Nat. Biotechnol.*, 1998, **16**, 49; (*c*) G. Bonnet, S. Tyagi, A. Libchaber and F. R. Kramer, *Proc. Natl. Acad. Sci. U. S. A.*, 1999, **96**, 6171; (*d*) D. P. Bratu, B.-J. Cha, M. M. Mhlanga, F. R. Kramer and S. Tyagi, *Proc. Natl. Acad. Sci. U. S. A.*, 2003, **100**, 13308; (*e*) W. Tan, K. Wang and T. J. Drake, *Curr. Opin. Chem. Biol.*, 2004, **8**, 1, and references therein.
8 For recent studies on intracellular trafficking of mRNA using controlled amounts of FISH probes, see for example: (*a*) D. Fusco, E. Bertrand and R. H. Singer, *Prog. Mol. Subcell. Biol.*, 2004, **35**, 135, and references therein; (*b*) Y. Shav-Tal, X. Darzacq, S. M. Shenoy, D. Fusco, S. M. Janicki, D. L. Spector and R. H. Singer, *Science*, 2004, **304**, 1797.
9 (*a*) M. N. Stojanovic, P. de Prada and D. W. Landry, *ChemBioChem*, 2001, **2**, 411; (*b*) M. N. Stojanovic, T. E. Mitchell and D. Stefanovic, *J. Am. Chem. Soc.*, 2002, **124**, 3555; (*c*) M. N. Stojanovic and D. Stefanovic, *Nat. Biotechnol.*, 2003, **21**, 1069.
10 J. S. Hartig, I. Grüne, S. H. Najafi-Shoushtari and M. Famulok, *J. Am. Chem. Soc.*, 2004, **126**, 722.
11 For recent examples of "amplifiable" oligonucleotide reactions on DNA templates, see: (*a*) Y. Gat and D. G. Lynn, *Biopolymers*, 1998, **48**, 19; (*b*) A. Luther, R. Brandsch and G. von Kiedrowski, *Nature*, 1998, **396**, 245; (*c*) D. Albagli, R. Van Atta, P. Cheng, B. Huan and M. L. Wood, *J. Am. Chem. Soc.*, 1999, **121**, 6954; (*d*) J. Brunner, A. Mokhir and R. Kraemer, *J. Am. Chem. Soc.*, 2003, **125**, 12410; (*e*) H. Abe and E. T. Kool, *J. Am. Chem. Soc.*, 2004, **126**, 13980.
12 For recent reviews on allosteric DNA/RNAzymes, see: (*a*) G. A. Soukup and R. R. Breaker, *Trends Biotechnol.*, 1999, **17**, 469; (*b*) T. Kuwabara, M. Warashima and K. Taira, *Curr. Opin. Chem. Biol*, 2000, **4**, 669.
13 For examples of oligonucleotide control of DNA/RNAzyme activities, see: (*a*) H. Porta and P. M. Lizardi, *Biotechnology*, 1995, **13**, 161; (*b*) D. Y. Wang and D. Sen, *J. Mol. Biol.*, 2001, **310**, 723; (*c*) D. Y. Wang, B. H. Y. Lai and D. Sen, *J. Mol. Biol.*, 2002, **318**, 33; (*d*) D. Y. Wang, B. H. Y. Lai, A. R. Feldman and D. Sen, *Nucleic Acids Res.*, 2002, **30**, 1735; (*e*) see also ref. 9 and ref. 10.
14 S. Sando, T. Sasaki, K. Kanatani and Y. Aoyama, *J. Am. Chem. Soc.*, 2003, **125**, 15720.
15 (*a*) R. I. Amann, L. Krumholtz and D. A. Stahl, *J. Bacteriol.*, 1990, **172**, 762; (*b*) B. M. Fuchs, G. Wallner, W. Beisker, I. Schwippl, W. Ludwig and R. I. Amann, *Appl. Environ. Microbiol.*, 1998, **64**, 4973.
16 The four stem-forming base pairs adjacent to the GrAT site were varied and so chosen, based on the simulation of intrastrand base-pairing, as shown in Fig. 1a (CG, TA, CG, and GC), to make the probe least structured and hence most flexible in the absence of the target. This is in order to demonstrate that the lock strategy works to lower the off-target reactivity, even on such systems as this.
17 S. W. Santoro and G. F. Joyce, *Proc. Natl. Acad. Sci. U. S. A.*, 1997, **94**, 4262.
18 M. T. Record, E. S. Courtenay, D. S. Cayley and H. J. Guttman, *Trends Biochem. Sci.*, 1998, **23**, 190, and references therein.
19 For recent reports on structural analysis of nucleic acids in crowded intracellular environments; see for example: D. Miyoshi, S. Matsumura, S. Nakano and N. Sugimoto, *J. Am. Chem. Soc.*, 2004, **126**, 165, and references therein.
20 B. M. Fuchs, F. O. Glöckner, J. Wulf and R. I. Amann, *Appl. Environ. Microbiol.*, 2000, **66**, 3603.
21 It is well known that oligonucleotide probes readily enter the paraformaldehyde-fixed *E. coli* cells in the presence of SDS; see for example ref. 15.
22 In order to shed light on the fate of the target–probe complex target–**3**^{FRET} (Fig. 4), we carried out cell sensing in the presence of Na^+ in place of Mg^{2+} which was absolutely essential for cleavage. The idea behind this control run with no Mg^{2+} is that FRET-freed complex target–**3**^{FRET} has no chance of self-cleavage and hence no chance of turnover, thus exhibiting one-equivalent or stoichiometric fluorescence signal at best. Actually, the fixed *E. coli* cells washed with and incubated in hybridization buffer containing probe **3**^{FRET} (1 μM) and Na^+ (900 mM) indeed fluoresce but weakly than they do in the presence of Mg^{2+} (25 mM). On this Mg^{2+}/Na^+ criterion, it is most likely that the enhanced fluorescence in the Mg^{2+} case is due to multiple-turnover catalytic cleavage of the complex target–**3**^{FRET} with signal amplification (step d in Fig. 4), although full interpretation of the results is deferred until more information is available as to the uptake/leak-out properties of the full-length probe and its cleavage fragments.
23 The self-cleavage of the FRET probe **3**^{FRET} in homogenous solution is hardly affected by the helper ODNs.
24 H. Kawasaki, R. Onuki, E. Suyama and K. Taira, *Nat. Biotechnol.*, 2002, **20**, 376.